Organic Electronics 14 (2013) 2087–2092

Contents lists available at SciVerse ScienceDirect

Organic Electronics

journal homepage: www.elsevier.com/locate/orgel

Twistable nonvolatile organic resistive memory devices

Sunghoon Song [a,1], Jingon Jang [b], Yongsung Ji [a], Sungjun Park [a], Tae-Wook Kim [c], Younggul Song [b], Myung-Han Yoon [a], Heung Cho Ko [a], Gun-Young Jung [a], Takhee Lee [b,*]

[a] School of Materials Science and Engineering, Gwangju Institute of Science and Technology, 1 Oryong-Dong, Buk-Gu, Gwangju 500-712, Republic of Korea
[b] Department of Physics and Astronomy, Seoul National University, Gwanak-ro, Gwanak-gu, Seoul 151-747, Republic of Korea
[c] Soft Innovative Materials Research Center, Korea Institute of Science and Technology, 864-9 Eunha-ri, Bongdong-eup, Wanju-gun, Jeollabukdo 565-905, Republic of Korea

ARTICLE INFO

Article history:
Received 20 February 2013
Received in revised form 29 April 2013
Accepted 3 May 2013
Available online 17 May 2013

Keywords:
Organic memory
Twistable
Nonvolatile
Resistive memory

ABSTRACT

We fabricated an 8×8 cross-bar array-type organic nonvolatile memory devices on twistable poly(ethylene terephthalate) (PET) substrate. A composite of polyimide (PI) and 6-phenyl-C61 butyric acid methyl ester (PCBM) was used as the active material for the memory devices. The organic memory devices showed a high ON/OFF current ratio, reproducibility with good endurance cycle, and stability with long retention time over 5×10^4 s on the flat substrate. The device performance remained well under the twisted condition with a twist angle up to ~30°. The twistable organic memory device has a potential to be utilized in more complex flexible organic device configurations.

1. Introduction

Numerous studies have reported on organic-based electronic devices such as organic light-emitting diodes, transistors, photovoltaics, and nonvolatile memories since the discovery of conducting polymers [1–5]. These organic-based materials and devices have many merits due to their innovative potential for flexibility and their easy and low-cost large-scale fabrication achieved by spin-coating and roll-to-roll processes [3,6–17]. In particular, organic nonvolatile memory (ONVM) devices are being widely investigated for next-generation data storage applications [15,17–23]. Although ONVMs still require considerable development to enhance device performances in comparison to inorganic nonvolatile memory devices, recent reports on the flexibility of organic memory and other types of devices have demonstrated various possibilities in unconventional device applications [24–27]. In future electronics, flexibility will be a very important factor in the development and applications of foldable and wearable electronics. Many research groups have reported amazing results for active materials, electrodes, and integrated circuits in flexible electronics based on organic and inorganic materials [26,28–31]. In addition, our group recently reported on molecular-scale flexible electronics achieved using self-assembled monolayers [32].

Likewise, ONVMs will be important in flexible electronic device applications. There are multiple types of ONVMs, which are classified as ferroelectric [17,22,23], flash [15,23], and resistive type [23,33,34] organic memory devices based on their operating mechanisms and device structures [23]. Among these types, resistive type memory devices have advantages such as lower operating voltages and simpler device structures. We recently reviewed some of the existing organic resistive memory devices in terms of performance enhancement and architectural issues, including the one transistor–one resistor (1T–1R)-type memory, the one diode–one resistor (1D–1R)-type memory, three-dimensionally integrated memory, and flexible memory [24,25,33–36]. Until now, most reports on flexible

* Corresponding author. Tel.: +82 2 880 4269; fax: +82 2 884 3002.
E-mail address: tlee@snu.ac.kr (T. Lee).
[1] Current Address: Samsung Electronics, 95, Samsung 2-ro, Giheung-Gu, Yongin-si, Gyeonggi-do 446-811, Republic of Korea (E-mail address: sh8008.song@samsung.com)

1566-1199/$ - see front matter © 2013 Elsevier B.V. All rights reserved.
http://dx.doi.org/10.1016/j.orgel.2013.05.003

memory devices have focused on bending conditions. However, such devices should be flexible in a variety of mechanically deformed configurations. For example, flexible devices should be not only bendable but also twistable or stretchable if possible. Thin and wavy Si-based foldable or stretchable electronic devices that are embedded in or deposited on poly(dimethylsiloxane) (PDMS) have been widely reported for various mechanical modification conditions [28,31,37].

In this work, we report the results of a study on the switching characteristics of organic resistive memory devices on a flexible substrate that was twisted to various degrees. A composite of polyimide (PI) and 6-phenyl-C61 butyric acid methyl ester (PCBM) was used as the active material of our resistive memory, as in our previous studies [24,34,35]. PI and PCBM composite materials have shown chemical and mechanical robustness and good thermal stability [35]. We fabricated PI:PCBM organic memory devices on flexible and twistable poly(ethylene terephthalate) (PET) substrates. The device parameters were characterized according to the degree of twisting, up to a twist angle of approximately 30°. We found that the statistical threshold voltage distribution and the ON/OFF current level remained well regardless of the degree of twisting, indicating the stability of the electrical characteristics of our memory devices under twisting stress. Moreover, reliable memory performance in terms of endurance cycles and retention time was demonstrated under twisting conditions.

2. Experimental section

To produce twistable organic memory devices on a PET substrate, the PET substrate was first cleaned by the typical ultrasonic cleaning process using acetone and IPA for 5 min, respectively. The bottom electrodes were deposited with eight lines of a 100-μm line-width pattern using a shadow mask by a thermal evaporator with the deposition rate of 5 Å/s at a pressure of $\sim 10^{-7}$ torr (Fig. 1a). The deposited metal consisted of Al (70 nm thickness) and the surface of the Al bottom electrodes was exposed to UV–ozone treatment for 10 min. Note that the surface of the Al bottom electrodes may contain the native Al oxide layer. The thin Al oxide layer may enhance the reliability of the organic resistive memory devices [38,39]. To prepare an active layer for the organic resistive memory, we used biphenyltetracarboxylic acid dianhydride p-phenylene diamine (BPDA–PPD) as a PI precursor; the BPDA–PPD was dissolved in N-methyl-2-pyrrolidone (NMP) solvent (BPDA–PPD:NMP solvent = 1:3 weight ratio). The 6-phenyl-C61 butyric acid methyl ester (PCBM) was dissolved in NMP solvent at a concentration of 0.5 wt%. Then, a PI:PCBM composite solution was prepared by mixing the PI solution (2 ml) with the PCBM solution (0.5 ml) and the PI:PCBM composite solution was spin-coated onto the Al electrodes/PET substrate at 500 rpm for 5 s and subsequently at 2000 rpm for 35 s (Fig. 1b). The coated film was soft-baked at 60 °C on a hotplate for 10 min in a N_2-filled glove box to dry and harden the deposited organic active layer. After the baking step, the bottom electrode pads were exposed by rubbing with a methanol-soaked swab for electrical probing (Fig. 1c). Next, we hard-baked the memory devices in a vacuum oven at 110 °C for 24 h to enhance the film uniformity, evaporate the residual solvent, and perform thermal curing. The thickness of the PI:PCBM composite active layer was measured at $\sim$60 nm by transmission electron microscopy (TEM) analysis. Finally, we deposited the top electrodes at a thickness of 70 nm crosswise to the bottom electrodes (Fig. 1d). Fig. 1f shows a photographic image of the completely fabricated our twistable organic memory devices.

Fig. 2a shows a cross-sectional TEM image of an organic memory cell. Good structural properties were observed by TEM; no agglomerations of the PCBM were observed in this image, indicating a good dispersion of the PCBM in the PI. Furthermore, aluminum was found to be absent in the organic active layer by the energy dispersive X-ray spectroscopy (EDS) data (Fig. 2b). The accidental penetration of Al elements would create filamentary paths and short out the memory cell. Carbon elements were mainly detected

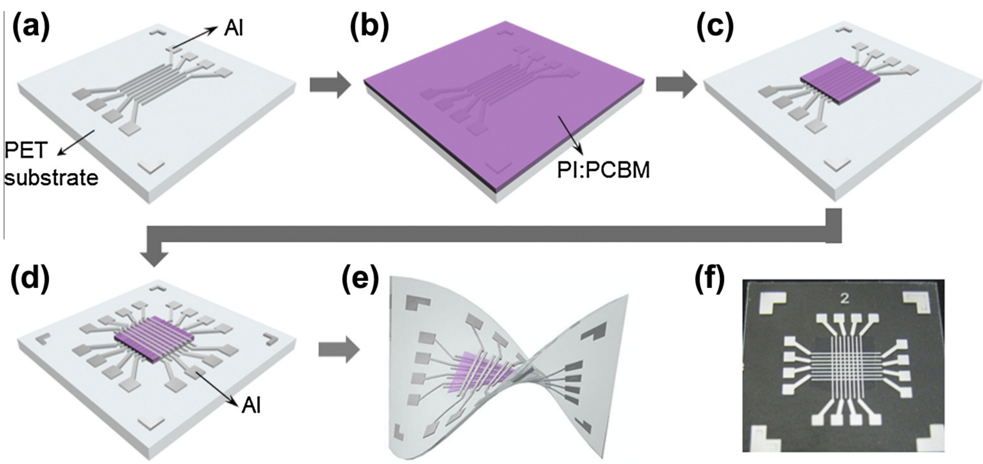

Fig. 1. (a–d) The fabrication process of the Al/PI:PCBM/Al organic resistive memory devices in an 8 × 8 array structure on a PET substrate. (e) Schematic illustration of twisted organic resistive memory devices. (f) A photographic image of the fabricated organic memory devices under the flat condition.

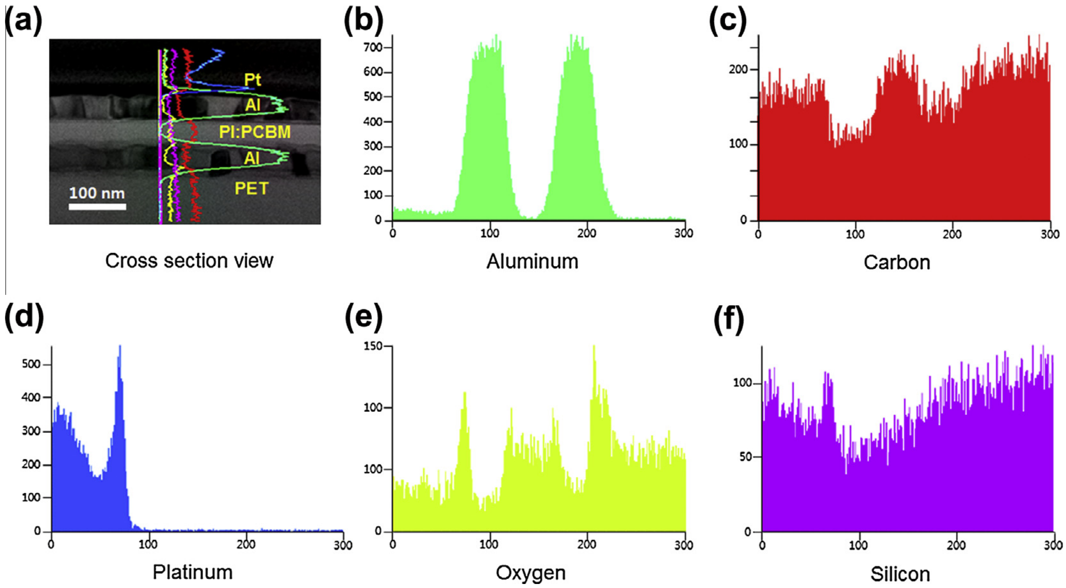

Fig. 2. (a) Cross-sectional TEM image of an organic memory device. The device was diced with a focused ion beam. (b–f) TEM EDS element profiles of an organic memory device. Each profile exhibits different color according to the different element (aluminum, carbon, platinum, oxygen, and silicon) contained in the total layer. (For interpretation of the references to color in this figure legend, the reader is referred to the web version of this article.)

in the organic active layer and the PET substrate (Fig. 2c). These results imply that the layers are well-separated and the resistive switching of our memory devices mainly functions in the PI:PCBM active layer.

3. Results and discussion

As shown in Fig. 3a, the electrical measurements of twistable organic memory devices were conducted using a semiconductor analyzer system (Model 4200-SCS, Keithley, Inc.) at room temperature in a N_2-filled glove box. Our memory devices exhibited well-defined memory-switching characteristics. The current–voltage (*I–V*) switching characteristics of our memory devices are shown in Fig. 3b. We applied a voltage from 0 to 7 V using a double sweep measurement. The initial state of the memory device was a high-resistance state (HRS, the OFF state). When the applied voltage exceeded 4.2 V, the OFF state of the

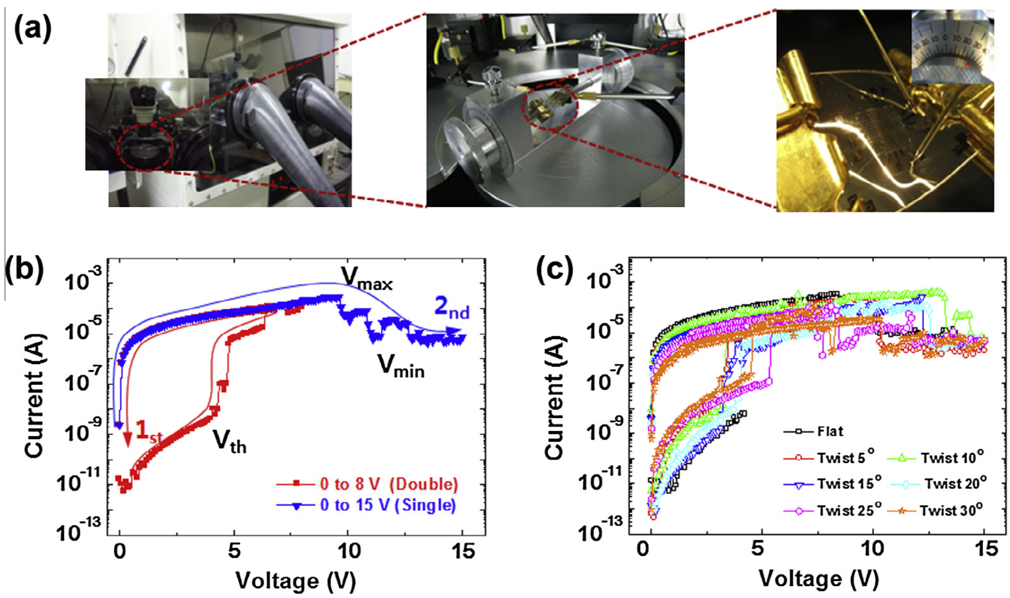

Fig. 3. (a) Photographic images showing the measurement of the organic memory devices under twisting using a probe station in a N_2-filled glove box. (b) Representative *I–V* curve of the fabricated organic memory devices under the flat condition. (c) *I–V* curves measured under various angles of twist from flat to a 30° twist angle.

memory device was abruptly changed to a low-resistance state (LRS, the ON state). Subsequently, when the voltage was decreased back to 0 V, the device remained in the ON state. This result reflects a nonvolatile memory characteristic. To turn off the device, the applied voltage was swept from 0 to 15 V; the device tracked the previous current characteristics of the ON state, and the device was turned off after ~11 V. We also observed a negative differential resistance (NDR) region between 9 and 13 V. The memory switching behavior shown in Fig. 3b is called unipolar type. Unipolar switching is achieved by the successive application of voltages with the same polarity [40]. These resistive switching characteristics can be explained by the charge-trapping mechanism proposed by Simmons and Verderber [41] and Bozano et al [42,43].

To verify whether our memory devices exhibited reliable switching characteristics under twisted conditions, we performed *I–V* measurements under twist conditions at various angles, as shown in Fig. 3c. During the twisting test, we twisted our organic memory devices from a flat condition to an angle of 30° with an increment angle of 5°. The memory characteristics were well maintained up to a 30° twist angle. Our organic memory devices did not exhibit reliable memory switching at a 35° twist angle; at that point, they showed a behavior of mixed ON and OFF states that could not be distinguished as reliable ON or OFF states. When we twisted beyond a 35° angle, we also observed irreversible failure of the memory devices. Therefore, we concluded that 30° was the maximum stable twist angle for our devices. The memory devices exhibited highly similar switching characteristics under both flat conditions and maximum twist angle (30°) conditions. To validate the reversibility of the electrical properties of our twistable organic memory devices, we measured the electrical characteristics when the devices were returned to the original flat condition after twisting. The switching characteristics showed no significant changes after the twist test (Fig. 3c), indicating that the switching property of our memory devices is resilient under twisting stress. The ON/OFF current ratios were found to be over 10^3 at all twist angles up to 30°.

Fig. 4 illustrates the statistical data for the switching characteristics of all of the memory devices under three conditions: flat (black), 15° twist angle (red), and 30° twist angle (blue). Despite the loss of some memory devices, our twistable devices exhibited a high device yield; specifically, all 64 devices operated well under the flat condition. Furthermore, 59 devices out of 64 (i.e., 92.2%) were operative as memory devices in the 15° twist angle condition, and 56 devices (i.e., 87.5%) were operative as memory devices in the 30° twist angle condition. These results suggest that a twisted organic memory device is possible, enabling the integration of twisting cross-bar type organic nonvolatile resistive memory devices. Fig. 4a shows the cumulative probability of the switching currents for all of the operative memory devices under three conditions: flat (black), 15° twist angle (red), and 30° twist angle (blue). Here, the current values were measured at a read voltage of 0.3 V and are plotted as the ON and OFF currents. The distribution of the ON current values is observed to lie within approximately two orders of magnitude, while the distribution of the OFF current values is somewhat broader. However, the important point is that the ON and OFF currents of our twistable memory devices are well separated by more than three orders of magnitude in both flat and twist conditions. Fig. 4b displays the statistical distributions of the threshold voltages (*V*th) of the operative memory devices under flat and twist conditions. The threshold voltage is the value at which the memory device switches to ON. As shown in Fig. 3b, the transition from the HRS to the LRS occurs at voltages between 3 and 7 V, which is a rather broad range. The distributions of the *V*th values were found to be similar for both the flat and twist conditions, indicating that all of the individual memory devices can be switched ON by a uniform parameter.

To examine in detail the memory performance of our twistable organic memory devices, we performed a series of characterizations, including a DC sweep endurance test and a retention test. As shown in Fig. 5a, the twisted organic memory devices exhibited good retention over a 5×10^4 s test period. In this retention test, the ON/OFF current ratios were also well maintained over four orders of magnitude and did not exhibit any serious electrical degradation under the three conditions: flat (black), 15° twist angle (red), and 30° twist angle (blue). Here, the current values of the two states (ON and OFF) were measured at a read voltage of 0.3 V. Fig. 5b–d show the results of the DC sweep endurance test for the three conditions. DC volt-

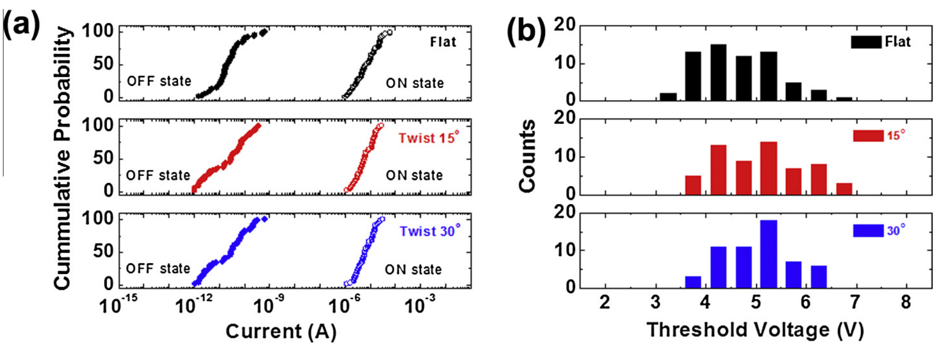

Fig. 4. Statistical data on the switching characteristics of all of the memory devices under three conditions: flat (black color), 15° twist angle (red color), and 30° twist angle (blue color). (a) Cumulative probability of the switching currents of all of the operative memory devices under the three conditions. (b) Threshold voltage distribution of the switching currents of all of the operative memory devices under the three conditions. (For interpretation of the references to color in this figure legend, the reader is referred to the web version of this article.)

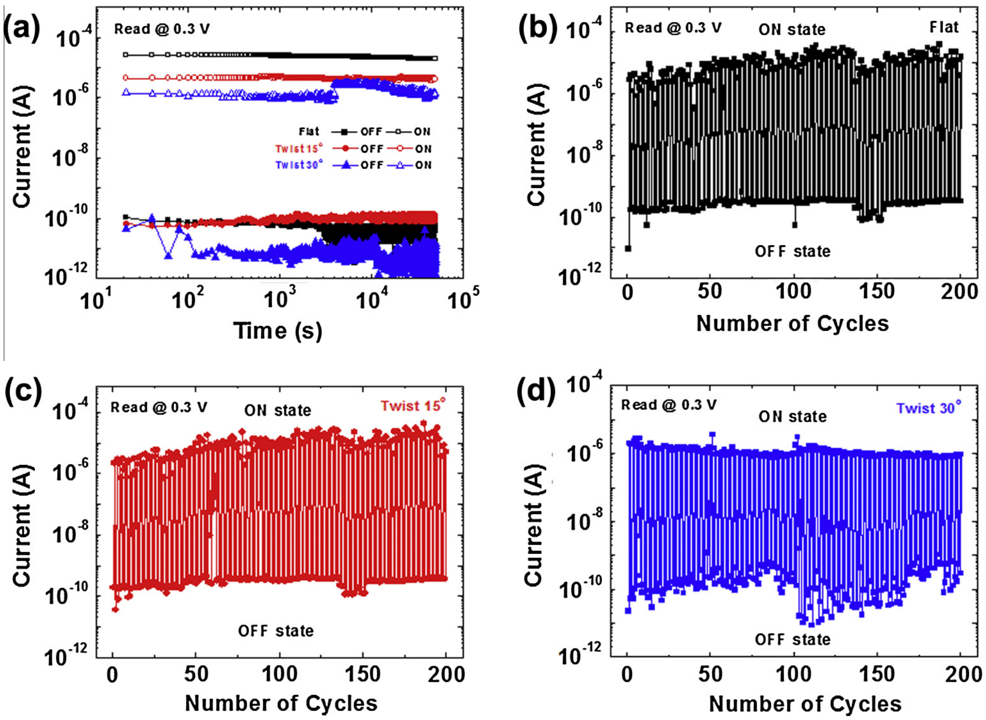

Fig. 5. (a) Retention times of the twistable organic memory devices under the three conditions: flat (black color), 15° twist angle (red color), and 30° twist angle (blue color). (b–d) DC sweep endurance test of the twistable organic memory devices under the three conditions. (For interpretation of the references to color in this figure legend, the reader is referred to the web version of this article.)

age sweeps were performed approximately 200 times using the same parameters for the memory devices under both flat and twist conditions. During the repetitive sweeps, our twistable memory devices maintained ON/OFF ratios of over $\sim 10^4$ without showing any significant electrical degradation. As demonstrated in our previous study, these reliable electrical performances highlight the potential for device application, which is strongly related to the possibility of three-dimensional stacking on flexible and twistable substrates [35].

4. Conclusions

In summary, we investigated the switching characteristics of 8×8 cross-bar array-type organic resistive memory devices on a PET twistable plastic substrate. A composite of PI and PCBM was used as the active material for the memory devices. Various device parameters were characterized over different twist angles. We found that the ON/OFF current cumulative probabilities were well separated regardless of the degree of twisting, up to a maximum twist angle of approximately 30°, indicating stable electrical characteristics of our memory devices under twisting stress. Moreover, reliable memory performance in terms of endurance cycles and retention time was demonstrated under twist conditions.

Acknowledgements

The authors thank the National Creative Research Laboratory Program (Grant No. 2012026372) and the National Core Research Center (Grant No. R15-2008-006-03002-0) of the Korean Ministry of Education, Science, and Technology.

References

[1] P. Peumans, S. Uchida, S.R. Forrest, Nature 425 (2003) 158.
[2] S. Reineke, F. Lindner, G. Schwartz, N. Seidler, K. Walzer, B. Lüssem, K. Leo, Nature 459 (2009) 234.
[3] H. Yan, Z. Chen, Y. Zheng, C. Newman, J.R. Quinn, F. Dötz, M. Kastler, A. Facchetti, Nature 457 (2009) 679.
[4] R.J. Tseng, J. Huang, J. Ouyang, R.B. Kaner, Y. Yang, Nano Lett. 5 (2005) 1077.
[5] A.J. Heeger, S. Kivelson, J.R. Schrieffer, W.-P. Su, Rev. Mod. Phys. 60 (1988) 781.
[6] T. Sekitani, H. Nakajima, H. Maeda, T. Fukushima, T. Aida, K. Hata, T. Someya, Nat. Mater. 8 (2009) 494.
[7] J.H. Oh, H.W. Lee, S. Mannsfeld, R.M. Stoltenberg, E. Jung, Y.W. Jin, J.M. Kim, J.-B. Yoo, Z. Bao, Proc. Natl. Acad. Sci. USA 106 (2009) 6065.
[8] T. Sekitani, Y. Noguchi, U. Zschieschang, H. Klauk, T. Someya, Proc. Natl. Acad. Sci. USA 105 (2008) 4976.
[9] H. Klauk, U. Zschieschang, J. Pflaum, M. Halik, Nature 445 (2007) 745.
[10] M.-H. Yoon, A. Facchetti, T.J. Marks, Proc. Natl. Acad. Sci. USA 102 (2005) 4678.
[11] Y.-Y. Noh, N. Zhao, M. Caironi, H. Sirringhaus, Nat. Nanotechnol. 2 (2007) 784.
[12] L. Herlogsson, Y.-Y. Noh, N. Zhao, X. Crispin, H. Sirringhaus, M. Berggren, Adv. Mater. 20 (2008) 4078.
[13] J.Y. Kim, K. Lee, N.E. Coates, D. Moses, T.-Q. Nguyen, M. Dante, A.J. Heeger, Science 317 (2007) 222.
[14] S.I. Na, S.-S. Kim, J. Jo, D.-Y. Kim, Adv. Mater. 20 (2008) 4061.
[15] T. Sekitani, T. Yokota, U. Zschieschang, H. Klauk, S. Bauer, K. Takeuchi, M. Takamiya, T. Sakurai, T. Someya, Science 326 (2009) 1516.
[16] C.-F. Sung, D. Kekuda, L.F. Chu, Y.-Z. Lee, F.-C. Chen, M.-C. Wu, C.-W. Chu, Adv. Mater. 21 (2009) 4845.
[17] T. Sekitani, K. Zaitsu, Y. Noguchi, K. Ishibe, M. Takamiya, T. Sakurai, T. Someya, IEEE Trans. Electron. Dev. 56 (2009) 1027.

[18] S. Möller, C. Perlov, W. Jackson, C. Taussig, S.R. Forrest, Nature 426 (2003) 166.
[19] Y. Yang, J. Ouyang, L. Ma, R.J.H. Tseng, C.W. Chu, Adv. Funct. Mater. 16 (2006) 1001.
[20] J.C. Scott, L.D. Bozano, Adv. Mater. 19 (2007) 1452.
[21] J.E. Green, J.W. Choi, A. Boukai, Y. Bunimovich, E. Johnston-Halperlin, E. Delonno, Y. Luo, B.A. Sheriff, K. Xu, Y.S. Shin, H.-R. Tseng, J.F. Stoddart, J.R. Heath, Nature 445 (2007) 414.
[22] R.C.G. Naber, K. Asadi, P.W.M. Blom, D.M. de Leeuw, B. de Boer, Adv. Mater. 22 (2010) 933.
[23] Q.D. Ling, D.-J. Liaw, C. Zhu, D.S.-H. Chan, E.-T. Kang, K.-G. Neoh, Prog. Polym. Sci. 33 (2008) 917.
[24] Y. Ji, B. Cho, S. Song, T.-W. Kim, M. Choe, Y.H. Kahng, T. Lee, Adv. Mater. 22 (2010) 3071.
[25] Y. Ji, S. Lee, B. Cho, S. Song, T. Lee, ACS Nano 5 (2011) 5995.
[26] T. Sekitani, U. Zschieschang, H. Klauk, T. Someya, Nat. Mater. 9 (2010) 1015.
[27] S. Kim, J.-S. Lee, Nano Lett. 10 (2010) 2884.
[28] J.A. Rogers, T. Someya, Y. Huang, Science 327 (2010) 1603.
[29] M. Park, J. Im, M. Shin, Y. Min, J. Park, H. Cho, S. Park, M.-B. Shim, S. Jeon, D.-Y. Chung, J. Bae, J. Park, U. Jeong, K. Kim, Nat. Nanotechnol. 7 (2012) 803.
[30] L. Hu, H.S. Kim, J.-Y. Lee, P. Peumans, Y. Cui, ACS Nano 4 (2010) 2955.
[31] A.C. Siegel, D.A. Bruzewicz, D.B. Weibel, G.M. Whitesides, Adv. Mater. 19 (2007) 727.
[32] S. Park, G. Wang, B. Cho, Y. Kim, S. Song, Y. Ji, M.-H. Yoon, T. Lee, Nat. Nanotechnol. 7 (2012) 438.
[33] T.-W. Kim, H. Choi, S.-H. Oh, G. Wang, D.-Y. Kim, H. Hwang, T. Lee, Adv. Mater. 21 (2009) 2497.
[34] B. Cho, T.-W. Kim, S. Song, Y. Ji, M. Jo, H. Hwang, G.-Y. Jung, T. Lee, Adv. Mater. 22 (2010) 1228.
[35] S. Song, B. Cho, T.-W. Kim, Y. Ji, M. Jo, G. Wang, M. Choe, Y.H. Kahng, H. Hwang, T. Lee, Adv. Mater. 22 (2010) 5048.
[36] B. Cho, S. Song, Y. Ji, T.-W. Kim, T. Lee, Adv. Funct. Mater. 21 (2011) 2806.
[37] D.-H. Kim, J.-H. Ahn, W.M. Choi, H.-S. Kim, T.-H. Kim, J. Song, Y.Y. Huang, Z. Liu, C. Lu, J.A. Rogers, Science 320 (2008) 507.
[38] F. Verbakel, S.C.J. Meskers, R.A.J. Janssen, H.L. Gomes, M. Cölle, M. Büchel, D.M. de Leeuw, Appl. Phys. Lett. 91 (2007) 192103.
[39] B. Cho, S. Song, Y. Ji, T. Lee, Appl. Phys. Lett. 97 (2010) 063305.
[40] B. Cho, T.-W. Kim, M. Choe, G. Wang, S. Song, T. Lee, Org. Electron. 10 (2009) 473.
[41] J.G. Simmons, R.R. Verderber, Proc. R. Soc. London, Ser. A 301 (1967) 77.
[42] L.D. Bozano, B.W. Kean, V.R. Deline, J.R. Salem, J.C. Scott, Appl. Phys. Lett. 84 (2004) 607.
[43] L.D. Bozano, B.W. Kean, M. Beinhoff, K.R. Carter, P.M. Rice, J.C. Scott, Adv. Func. Mater. 15 (2005) 1933.